J Water Environ Nanotechnol 2026, 11(3): 345-362
10.22090/jwent.2026.2089188.2134

RESEARCH PAPER

Comparative Analytical Performance of Magnetic ZnO-Modified Activated Carbons Derived From Ziziphus Spina-Christi and Cordia Myxa Seeds for the Removal of Cd(II) and Ni(II) Ions From Aqueous Solutions

Wijdan Adnan Hasan *, Nisreen Abdulkareem Abdulaali

Department of Chemistry, College of Science, University of Misan, Maysan, Iraq.

*Corresponding Author(s)
Email:
wijdan@uomisan.edu.iq

Article History:
Received: 2026-05-31
Revised: 2026-07-31
Accepted: 2026-08-08

HIGHLIGHTS

- Sustainable preparation of magnetic ZnO-modified activated carbons from Ziziphus spina-christi and Cordia myxa seeds.
- The composites prepared had a high effective capability for the removal so as to reduce ions of Cd(II) and Ni(II) ions.
- The adsorption performance was closely related to the solution pH, initial metal concentration, and contact time.
- The magnetic ZnO/activated carbon composites were characterized by XRD, FTIR, SEM–EDS, and BET analyses.
- The prepared bio-sorbents offer an eco-friendly and economically effective method of treating water.

ABSTRACT

Growing discharge of harmful heavy metals into aquatic ecosystems has prompted an ever-expanding effort to discover effective, viable, and low-cost adsorbents for water treatment. Using the hydrothermal synthesis method, this study successfully prepared and modified activated carbons from Ziziphus spina-christi (ZAC) and Cordia myxa (CAC) seeds with magnetic zinc oxide nanoparticles (MZnO). Various mass ratios of activated carbon to MZnO were mixed to prepare composite adsorbents, where the 2:1 ratio showed the optimum adsorption capacity and was selected for further studies. Fourier transform infrared spectroscopy (FTIR), X-ray diffraction (XRD), scanning electron microscopy coupled with energy-dispersive X-ray spectroscopy (SEM–EDX), and zeta potential analysis were used to characterize the synthesized materials in detail. The characterization results confirmed that the magnetic ZnO nanoparticles can be successfully embedded into a porous activated carbon matrix while maintaining the functional groups responsible for metal ion adsorption. This study presents batch adsorption experiments to assess the removal of Cd(II) and Ni(II) ions at various operating conditions (initial metal ion concentration, contact time, solution pH). The maximum adsorption conditions were also realized at initial metal ion concentrations of 50 mg L^{-1}, contact time of 60 min for Cd and 120 for Ni for CAC/MZnO. The contact time was 150 min for Cd and 180 for Ni for ZAC/MZnO. and pH 6. The improved adsorption performance may be attributed to the combined contribution of the porous activated carbon framework and the active sites provided by the magnetic ZnO nanoparticles. The developed composites showed good adsorption capacity for both Cd(II) and Ni(II), indicating that they can be applied as an effective medium of environmentally friendly, easy-to-reprocess, efficient, and cheap adsorbents for treating heavy metal-polluted water.

The adsorption equilibrium of Cd(II) and Ni(II) was better fitted by the Langmuir isotherm than the Freundlich model. The highest adsorption capacity was achieved by ZAC/MZnO (2:1) for Cd(II) (qmax = 142.86 mg g^{-1}), followed by ZAC/MZnO for Ni(II) (116.90 mg g^{-1}), CAC/MZnO for Cd(II) (103.63 mg g^{-1}), and CAC/MZnO for Ni(II) (88.54 mg g^{-1}), confirming the superior adsorption efficiency of ZAC/MZnO.

KEYWORDS:

Activated Carbon; Ziziphus spina-christi; Cordia Myxa; Magnetic ZnO; Cd(II); Ni(II); Adsorption; Water Treatment.

How to cite this article
Adnan Hasan W and Abdulkareem Abdulaali N. Comparative Analytical Performance of Magnetic ZnO-Modified Activated Carbons Derived from Ziziphus spina-christi and Cordia myxa Seeds for the Removal of Cd(II) and Ni(II) Ions from Aqueous Solutions. J Water Environ Nanotechnol 2026, 11(3): 345-362, DOI: 10.22090/jwent.2026.2089188.2134

©2026 The Author(s). Published by the Iranian Environmental Mutagen Society. This work is licensed under the Creative Commons Attribution 4.0 International License (CC BY 4.0). To view a copy of this license, visit http://creativecommons.org/licenses/by/4.0/.

INTRODUCTION

Industrialization, mining processes, electroplating, battery production, metal finishing, and fertilizer application discharge heavy metals into aquatic environments at high levels [1]. In contrast to most organic contaminants, heavy metals are non-biodegradable, extremely persistent environmental pollutants, bioaccumulating through the food chain and causing serious ecological and human health hazards. Cadmium (Cd(II)) and nickel (Ni(II)) are widely regarded as principal contaminants due to their toxicity, bioaccumulation potential in the food chain pathways, and high mobility in aquatic environments since they remain stable ions in different aqueous environments. In the meantime, chronic exposure to cadmium induces kidney injury, osteoproductivity, and has been linked with a potential carcinogenic effect; additionally, high consumption of nickel can cause internal dermatitis as well as damage respiratory diseases and different systemic disorders. Therefore, it has become a major environmental priority to develop effective, low-cost and eco-friendly technologies for the removal of these toxic metals from water [2].

Several physicochemical methods have been established for the removal of heavy metals, such as chemical precipitation, ion exchange, membrane filtration, electrochemical treatment, coagulation-flocculation and solvent extraction. While these technologies can obtain high removal efficiencies of micro-pollutants under some operating conditions, they tend to be associated with disadvantages such as: (1) high operation cost, (2) complex process control, (3) high energy consumption and (4) generation of toxic sludge as secondary pollutants. On the other hand, adsorption has proved to be one of the most attractive water treatment technologies, relying on its simple operation and high removal efficiency with little capital costs, along with applicability to a large range of contaminant concentrations [3].

The specific surface area, pore structure, surface chemistry, and abundance of active functional groups of a material have an important impact on its adsorption performance. Owing to its highly porous structure and remarkably high adsorption capacity, activated carbon is still the most widely used adsorbent. Nevertheless, the high cost of commercially available activated carbon has stimulated researchers to explore low-cost alternatives based on biomass as raw materials, derived from agricultural waste. Transforming agricultural by-products into value-added adsorbents not only reduces production costs, but also helps in waste management and complements sustainable, environmentally friendly choices within the circular economy context [4].

Because of their high carbon content, lignocellulosic composition, low ash content and widespread availability, fruit seeds are an appealing biomass precursor for activated carbon development. The evolution occurs during the processes of carbonization and chemical activation, leading to an interconnected porous structure filled with oxygen-containing functional groups such as hydroxyl, carbonyl, and carboxyl functions that enable heavy metal adsorption through interactions via electrostatic attraction, ion exchange, surface complexation, and coordination. A variety of agricultural wastes, however, can serve as suitable precursors for advanced adsorbent materials; Ziziphus spina-christi seeds and Cordia myxa seeds, which are present in relatively large quantities across many Middle Eastern countries [5], despite their physicochemical characteristics being generally favorable, remain under-used. Recent studies have demonstrated the broad applicability of engineered nanomaterials and porous systems across biomedical and environmental fields. Superparamagnetic iron oxide nanoparticles have been investigated as carriers for antigen delivery [6]. It has also been combined with plant-derived compounds to enhance biological activity [7]. In addition, porous-gradient materials have been incorporated into microfluidic platforms for chemotaxis studies [8]. From an environmental perspective, plant species including *Ziziphus spina-christi* have shown measurable morphological responses to atmospheric pollutants, indicating their interaction with and sensitivity to surrounding environmental conditions [9].

Even though the activated carbon made from biomass has good adsorption properties, one of its drawbacks is that separating it from water treatment, in which it goes into a fine powder state, is difficult. The number of available active sites may also limit the adsorption capacity of raw activated carbon. To remedy these restrictions, a lot of efforts have been made in recent years to design nanocomposite adsorbents that introduce metal oxide nanoparticles on porous carbon matrices. These hybrid materials benefit both from the high surface area of activated carbon and novel physicochemical properties of nanomaterials, leading to exceeding adsorption efficiency and improved structural stability [10].

Zinc oxide (ZnO) is one of the most studied metal oxide nanoparticles owing to its chemical stability, environmental friendliness, low toxicity, and high affinity toward heavy metal ions. ZnO nanoparticles are rich in surface hydroxyl groups and oxygen vacancies that act as additional adsorption sites which can interact with dissolved metal ions through electrostatic attraction, complexation and ion-exchange mechanisms. However, one of the limiting factors in their application is a propensity to agglomerate when suspended in aqueous media and the difficulty with which the nanoparticles can be recovered directly after adsorption [11].

However, you overcome this restriction could be a formidable approach of magnetic modification. The utilization of magnetic iron oxide in ZnO nanoparticles facilitates rapid and effective adsorbent removal from treated water by means of an externally applied magnetic field, at the same time enhancing recyclability of the materials and constraining

secondary pollution. Moreover, the magnetic ZnO/activated carbon composite adsorbent becomes a multifunctional material by coupling the porous carbon framework with a high number of adsorption sites in connection with active surface centers from the combination of activated and non-activated material, together with magnetic properties assisting post-treatment recovery. The synergistic interplay between these units often demonstrates better adsorption behavior than the individual. Although dozens of research studies have focused on preparing biomass-derived activated carbons and novel magnetic nanocomposite adsorbents, few direct comparisons between the adsorption properties of activated carbons prepared from diverse fruit seed precursors following surface modification with magnetic ZnO nanoparticles are available. Additionally, very few studies have examined cadmium and nickel ion adsorption on magnetic ZnO-zinc oxide functionalized activated carbons derived from Ziziphus spina-christi (Z. spina-christi) and Cordia myxa seeds systematically under the same experimental conditions. Comparative studies are crucial to investigate how biomass precursor properties affect adsorption performance and whether the most suitable low-cost adsorbents can be selected for water remediation [12]

Recent investigations indicate that biomass-derived AC and magnetic nanocomposites may be more effective for heavy metal removal since they are more available and less costly than synthetic carbonaceous articles. Razali et al. (2022) [13] developed high-surface-area activated carbon from mango peels and seeds using hydrothermal synthesis and $ZnCl_2$ activation and showed that the concave: convex aspect ratio of 1 was an effective modality for designing highly porous adsorbents. Karapınar (2022) [14] examined mixed fruit seeds, and used $ZnCl_2$, KOH arid H_3PO_4 during chemical activation of activated carbon synthesizing pictures in water, with adsorptive capacities for Ni(II), Cr(III) and Cu(II) reached around 118.02 mg g^{-1}, 146.03 mg g^{-1} and 150.45 mg g^{-1} respectively study on heavy metal removal capability from aqueous solutions of commercial scale such as fruit-seed-derived activated carbons. Analogously, in a recent study, Salman et al. (2024) [15] produced microwave-activated carbon from plum seeds for co-removal of bimetal ions; they reported that the porous structure and adsorption performance of the prepared adsorbent were significantly improved by microwave activation. In another recent study Kusdarini et al. (2025) [3] synthesized magnetic activated carbon from snake fruit (Salacca zalacca) seeds coating that achieved a high Cd(II) removal of 80.12–87.75%, as well as a good correlation between the adsorption equilibrium and Langmuir isotherm model, which indicates the positive synergetic effects of integrating an efficient adsorbent material to enhance their separation ability while facilitating easy recovery by external magnetic fields. Furthermore, Kukowska et al. (2025) [16] elaborated the adsorption characteristics of activated carbons prepared from fruit wastes through hydrothermal synthesis activation towards metals and metalloids in aqueous multi-component systems, proposing an agricultural waste as a sustainable source for developing advanced adsorbents. While these studies have established the suitability of biomass-derived activated carbons and their magnetic composites for water treatment, there is still a lack of comparative studies in which magnetized ZnO-functionalized activated carbons made from various fruit seed precursors (especially Ziziphus spina-christi and Cordia myxa seeds) are employed to remove Cd(II) and Ni(II) ions in fixed mode under the same experimental conditions.

While many works have prepared activated carbon from various types of agricultural wastes and others studied ZnO-based adsorbents for heavy metal removal, little has been done on a comparative study of magnetic ZnO-modified activated carbons produced from different natural seed precursors in the same preparation and adsorption conditions. Additionally, a direct comparison of Ziziphus spina-christi and Cordia myxa seed-derived activated carbons following their magnetic ZnO modification for the simultaneous removal of Cd(II) and Ni(II) ions has not been studied enough. Hence, this study fills this research gap by providing a systematic comparison of the physicochemical properties and adsorption capabilities of these two inexpensive biosorbents.

Hence, the originality of this work lies in its design by comparing two different generations of magnetic ZnO-modified activated carbons obtained from Ziziphus spina-christi and Cordia myxa seed wastes. The attraction of this study lies in the full comparison of their adsorption performance for Cd(II) and Ni(II) ions, focused on the effect of biomass precursors on adsorbent efficacy and proving that these sustainable materials have promise as a material suitable for belittling water.

While great work has been done in biomass-based adsorbents for heavy metal removal, few are still performed between activated carbons prepared after magnetization with ZnO nanoparticles of different fruit seed precursors. In addition, no significant attention has been paid to investigating the adsorption performance of activated carbons derived from Ziziphus spina-christi– and Cordia myxa under similar experimental conditions toward Cd(II) and Ni(II) ions. Thus, a deeper understanding of how the characteristics of biomass precursors affect adsorption behaviour is needed for the development of efficient and sustainable adsorbents that can be recovered magnetically from water.

MATERIALS AND METHODS

Materials

Two types of biomass precursors, namely seeds of Ziziphus spina-christi (ZSC) and Cordia myxa (CM), were collected from Iraqi local markets for the purpose of activated carbon preparation. The chemicals in this work, zinc acetate dihydrate

J Water Environ Nanotechnol, 2026, 11(3): 345-362
10.22090/jwent.2026.2089188.2134

($Zn(CH_3COO)_2{\cdot}2H_2O$), urea ($CH_4N_2O$), polyethylene glycol (PEG-3500), ferric sulfate hydrate ($Fe_2(SO_4)_3{\cdot}xH_2O$), sodium hydroxide (NaOH), phosphoric acid (H_3PO_4), zinc chloride($ZnCl_2$) hydrochloric acid(HCl) ethanol and deionized water were used as the analytical grade before purification.

Cadmium nitrate tetrahydrate ($Cd(NO_3)_2{\cdot}4H_2O$) and nickel nitrate hexahydrate ($Ni(NO_3)_2 \cdot 6H_2O$) were used to create Cd(II) and Ni(II), respectively, stock solutions. Dilutions in deionized water were performed to obtain working solutions in the desired concentrations.

Preparation of Activated Carbon

Activated Carbon Derived from Ziziphus spina-christi Seed (ZAC)

Collected seeds were carefully washed in distilled water to remove dust and contaminants, allowed to be oven-dried at 110°C, and ground into fine powder. The powdered material was chemically doped with phosphoric acid and then underwent impregnation followed by carbonization. The impregnated biomass was then carbonized in a muffle furnace for 2 h at 500 °C. The carbon was rinsed several times with distilled water until

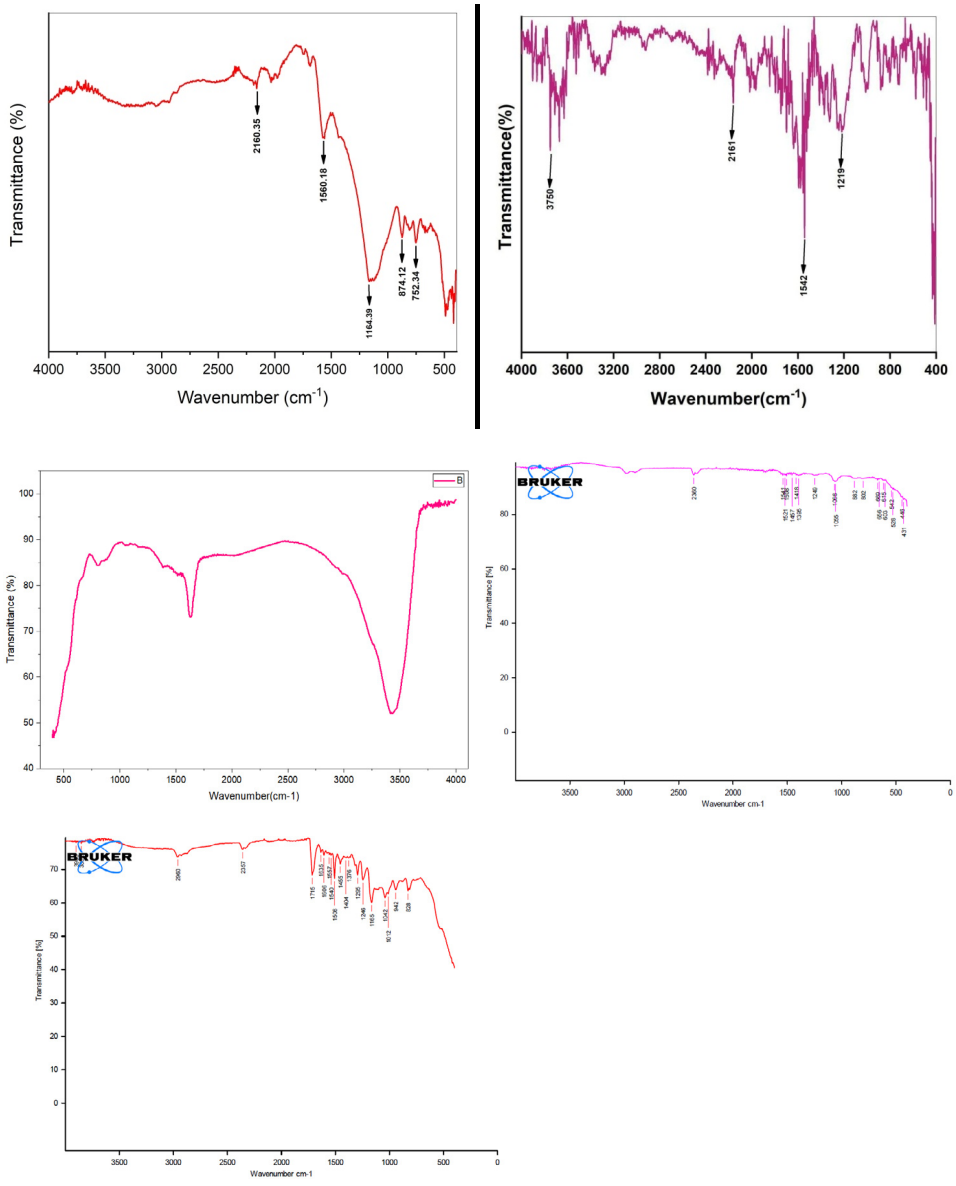

Fig. 1. Fourier transform infrared (FTIR) spectra of the prepared adsorbents: (a) activated carbon derived from Ziziphus spina-christi seeds (ZAC), (b) activated carbon derived from Cordia myxa seeds (CAC), (c) magnetic zinc oxide nanoparticles (MZnO), (d) ZAC/MZnO composite (2:1), and (e) CAC/MZnO composite (2:1).

the pH of the washing solution reached nearly neutral (6–6.5) and then dried, ground into powder to yield activated carbon (ZAC) [17].

Activated Carbon Derived from Seeds of Cordia myxa (CAC)

Suspensions of the Cordia myxa seeds were obtained by washing, drying, and mechanically grinding the seeds; The carbonized powder biomass in a nitrogen atmosphere at 450–500 °C was immersed for 2 h in 0.5 M HCl to remove inorganic impurities, thoroughly washed with distilled water until neutral pH, and finally dried at 105 °C [18]. Afterwards, the chemical activation was performed by following two steps: impregnation of the Cordia myxa with ZnCl2, intermediate washing, and drying to prepare RAW AC (CAC).

Synthesis of ZnO Nanoparticles

Then, dissolve 1 g of PEG into 20 mL of water, and then add 2.19 g Zn(CH3CO2)2.2H2O salt. A 0.5 M urea solution (20 mL) was added. This mixture was then put into 50 mL Teflon-lined stainless steel autoclaves and heated in an oven at 150 ^{0}C for 12 hours. The precipitate was washed with distilled water and ethanol after the reaction, followed by drying at 80 ^{0}C for 12 hours, as the temperature decreased spontaneously to room temperature. The solid produced was then heated in a muffle furnace at 350 ^{0}C over a period of 2 hours (heating rate of 2 ^{0}C/min). [19].

Preparation of Magnetic ZnO Nanoparticles

In a beaker, place 0.2 g of ZnO in 20 mL of deionized water in an ultrasonic bath. A different beaker containing 0.328 g of FeSO4 is then Dissolved 7H2O in 20 mL of DI water. 2.1 g of NaOH was added to it and was stirred for 10 min. And the received solution was poured onto ZnO. After that, carried into a 50 mL Teflon-lined stainless steel autoclave and kept at 150 ^{0}C for 12 hours. The red-brown precipitate formed was collected by centrifugation (8000 rpm, 20 min) and repeatedly washed with deionized water and absolute ethanol. To obtain the same iron oxide components but with higher concentrations of ZnO, the precipitate was aged at 80 ^{0}C for 12 hours (ZnO@Fe3O4-1:1) [20,21].

Characterization of the Adsorbents

Characterization: The synthesis of the magnetically separated activated carbons and magnetic ZnO nanoparticle or carbon composites was characterized using different characterization techniques. Materials adsorbent scavenger via one-pot hydrothermal synthesis route/ Activation channels v 1. Surface Functional Group Identification –FTIR (Fourier Transform Infrared Spectroscopy) FTIR was used to identify the presence of functional groups on the surface. Crystalline phases were determined by X-ray Diffraction (XRD). Surface morphology and elemental composition were measured by scanning electron microscopy/EDX (SEM–EDX). Zeta potential measurements were performed to evaluate surface charge characteristics.

Batch Adsorption Experiments

The adsorption capacities of the prepared ZAC/MZnO and CAC/MZnO on Cd(II) and Ni(II) ions were investigated by batch experiments. The aqueous solutions used in this study were prepared with the following initial metal ion concentrations: 10, 25, 50, 100,150 and 200 mg/L. In each experiment, a metal ion solution of 25 mL was placed in the conical flask, and 0.025 g of prepared adsorbent was added. For equilibration of the mixtures, these were shaken at room temperature (24 h) at 300 rpm. Centrifugation was used to separate the suspensions again after equilibrium, and Atomic Absorption Spectroscopy (AAS) was utilized to determine the residual concentrations of Cd(II) & Ni(II) ions in the supernatant. The adsorption capacity at equilibrium (q_e, mg g^{-1}) was determined by the following equation:

$$q_e = \frac{(C_\circ - C_e)V}{m} \quad \text{... [22]}$$

where $\mathbf{C_0}$ (mg L^{-1}) is the initial concentration of the metal ion, $\mathbf{C_e}$ (mg L^{-1}) is the equilibrium concentration, **V** (L) is the volume of the solution, and **m** (g) is the mass of the adsorbent.

Determination of Metal Ion Concentration

Before and after adsorption, Atomic Absorption Spectroscopy (AAS) was used to measure the concentrations of Cd(II) and Ni(II) ions. Standard calibration solutions of each individual metal ion were then prepared over the relevant concentration range, plotting absorbance against concentration to give calibration curves. These calibration curves were found to be highly linear and can thus be used to measure the residual concentrations of Cd(II) and Ni(II) ions from the adsorption experiments.

RESULTS AND DISCUSSION

Characterization of the Prepared Adsorbents

FTIR Analysis

The FTIR spectra of the prepared activated carbons from Ziziphus spina-christi (ZAC) and Cordia myxa (CAC), and magnetic ZnO nanoparticles (MZnO) as well as their composites (ZAC/MZnO, CAC/MZnO) are shown in Figure 1. The spectra provide important information on the surface functional groups in charge of adsorbing metal ions and at the same time verify that magnetic ZnO nanoparticles were introduced onto the activated carbon matrix.

The ZAC FTIR spectrum (Fig. 1a) demonstrated a wide absorption band within the 3200-3500 cm^{-1} region, which can usually be assigned to the stretching vibration of hydroxyl (-OH) groups derived from combined absorbed moisture and

J Water Environ Nanotechnol, 2026, 11(3): 345-362
10.22090/jwent.2026.2089188.2134

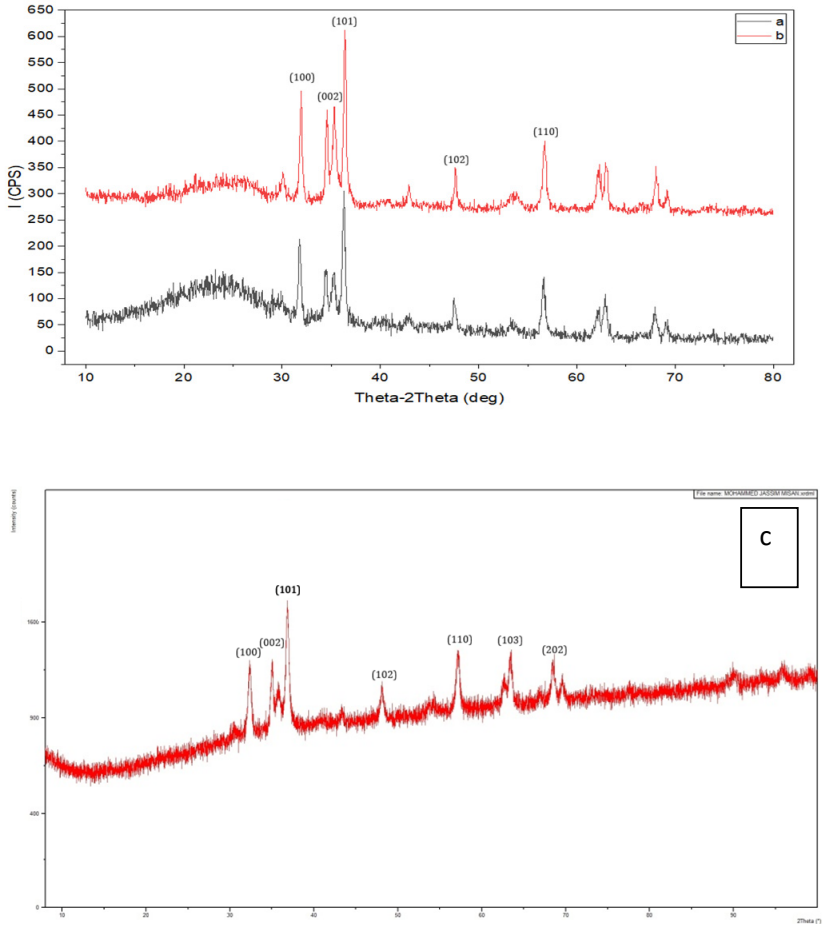

Fig. 2. X-ray diffraction (XRD) patterns of the prepared adsorbents: **(a)** CAC/MZnO (2:1) composite, **(b)** ZAC/MZnO (2:1) composite, and **(c)** magnetic ZnO nanoparticles (MZnO).

phenolic functionalities. A weak absorption band appears around 2160 cm−1. Bands at ratios of approximately 874 and 752 cm^{-1} are attributed to C–H out-of-plane bending vibrations in the presence of aromatic C, suggesting that these structures are generated by the carbonization process development. The oxygen-containing functional groups are supposed to act as active spots for the adsorption of heavy metal ions via complexation and electrostatic interactions [23].

As shown in Fig. 1b) also exhibited characteristic bands from oxygen-containing functional groups. The wide band around 3750 cm^{-1} corresponds to hydroxyl stretching vibrations. The weak peak found around 2161 cm^{-1} might be attributed to the C=C stretching vibration of unsaturated carbon species. There is a strong absorption band at 1542 cm^{-1} associated with aromatic C=C stretching and/or carbonyl-related functional groups, as well as a peak at 1219 cm^{-1} corresponding to the C–O stretching vibrations of alcohols, phenols, or carboxylic groups. This implies that CAC has chemically reactive sites that can interact with dissolved metal ions during the adsorption process, as the oxygenated surface functionalities are present.

FTIR characterization of MZnO. The FTIR spectrum of MZnO (Fig. 1c) showed a broad absorption band at around 3429 cm^{-1} assigned to the stretching vibration of surface hydroxyl groups. The absorbance band in the range near 1629 cm^{-1} is attributed to this bending vibration of physically adsorbed water molecules. A characteristic of successful magnetic ZnO nanoparticle preparation is a strong absorption band below 500 cm^{-1}, around 410 cm^{-1}, which is assigned to metal–oxygen (Zn–O and Fe–O) stretching vibrations [24].

FTIR Spectra of composite adsorbents: (ZAC/MZnO; B) CAC/MZnO 1d and Fig. 1e, respectively. When compared with the pure activated carbons, most characteristic absorption bands experienced small shifts of their band positions, combined with great changes in intensity. The bands due to the metal–oxygen vibrations, appearing below 600 cm^{-1}, were clearly increased after composite formation, which confirms that the magnetic

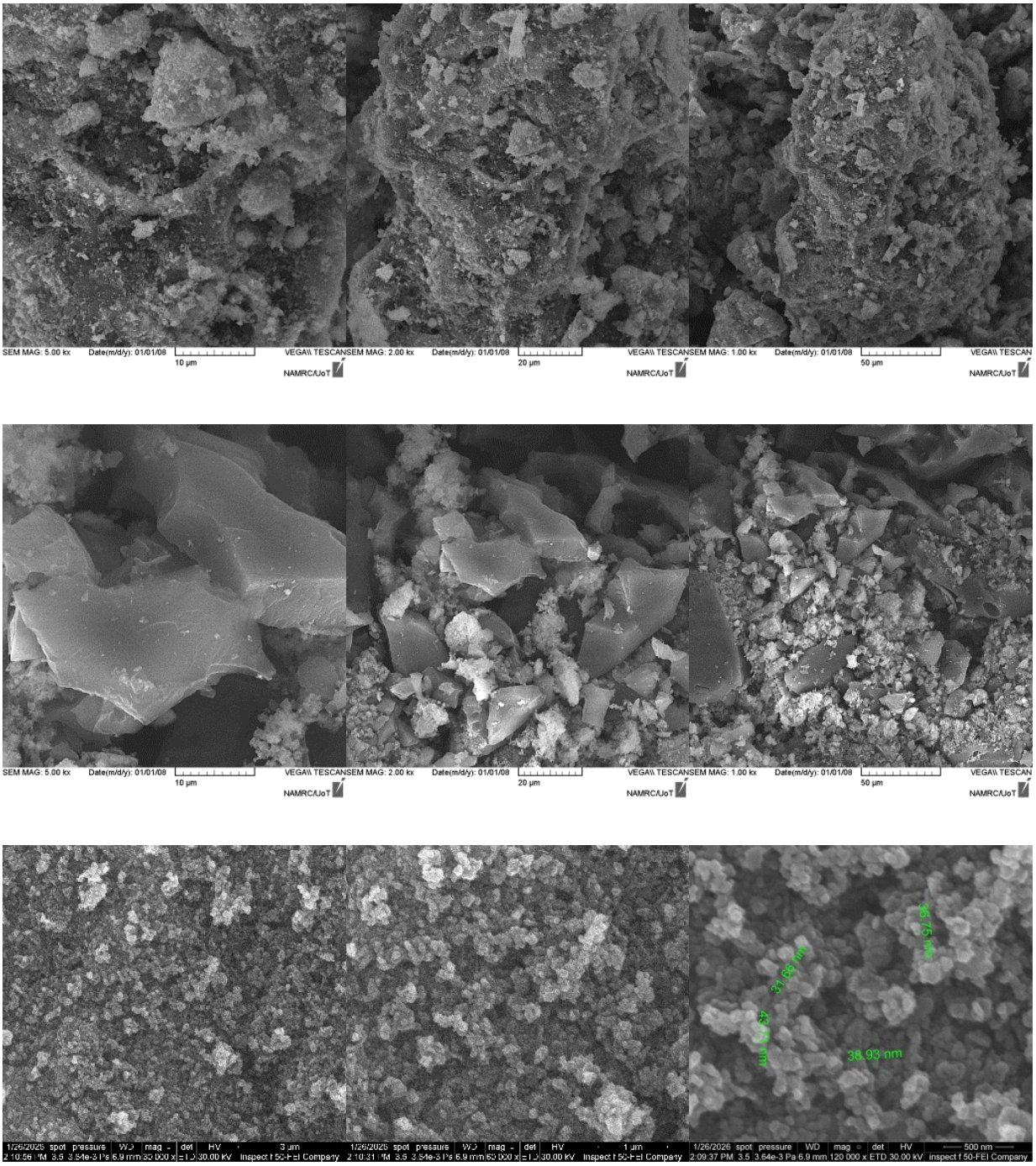

Fig. 3. SEM micrographs of the synthesized adsorbents at different magnifications: (a) CAC/MZnO (2:1) composite, (b) ZAC/MZnO (2:1) composite, and (c) magnetic ZnO nanoparticles (MZnO).

ZnO nanoparticles screened successfully on the activated carbon surface. In addition, the finding of oxygen-containing functional groups of activated carbon after modification indicates that the chemical activation process mainly kept the adsorption-active functional groups, with some additional ZnO and FeO active sites being introduced in place. Linking the coexistence of hydroxyl, carbonyl, ether, and metal oxide functional groups on activated carbon will work together to improve its adsorption

J Water Environ Nanotechnol, 2026, 11(3): 345-362
10.22090/jwent.2026.2089188.2134

performance through various interaction mechanisms between adsorber surface and Cd(II)/Ni(II) ions (e.g., electrostatic attractive interaction, surface complexation, ion exchange, et al.

In summary, the FTIR results agree well with the successful preparation of magnetic ZnO-modified activated carbon composites and do not result in destruction of surface functional groups needed to improve physicochemical characteristics of biomass-derived activated carbons. Because there are numerous oxygen-containing functionalities in such a hybrid, together with magnetic metal oxide active sites, it is expected that these functional moieties will allow plenty of adsorption centers to adsorb heavy metal ions from the aqueous solution. [25].

XRD Analysis

The XRD patterns of the magnetic ZnO nanoparticles (MZnO), ZAC/MZnO (2:1), and CAC/MZnO (2:1) composite samples are shown in Fig. 2. The crystalline structure of the obtained materials and the successful incorporation of magnetic ZnO nanoparticles into activated carbon matrices were analysed by XRD.

The MZnO powder consists of a diffraction pattern in Fig 2. As shown in Fig. 2c), prominent diffraction peaks appearing at around 31.8°, 34.4°, 36.2°, 47.5°, 56.6°, 62.8° and,67.9° (2θ) were characteristic reflections of the hexagonal wurtzite ZnO crystal structure, which can be indexed to the (100), (002), (101), (102), (110), (103) and, (112) crystallographic plane, respectively. The broad range with high intensity and high sharpness of these reflections implies the success of the formation of highly crystalline ZnO nanoparticles. Further evidence for the successful magnetic modification of ZnO is also due to weak diffraction peaks associated with magnetic iron oxide [26], which do not significantly change the crystal structure of the host only.

The XRD pattern of the ZAC/MZnO (2:1). The pattern of 2b) showed that all the characteristic peaks corresponding to crystalline ZnO are retained, suggesting that the crystal structure of the nanoparticles was preserved after immobilization onto the activated carbon surface. A broad diffraction halo observed in the region of about 20–26° (2θ) is associated with the amorphous carbon structure of activated carbon prepared from seeds of Ziziphus spina-christi compared with pure MZnO. Additionally, the intensity of the ZnO diffraction peaks decreased significantly due to a homogeneous dispersion of magnetic ZnO nanoparticles into the porous carbon framework and because they are partially shielded by its amorphous carbon matrix.

Correspondingly, the X-ray diffraction data of the CAC/MZnO (2:1) composite (Fig. 2a) showed the reflections characteristic of crystalline ZnO with the broad amorphous characteristic carbon band in between 20 and 30°(2θ). The absence of extra out-of-place diffraction peaks associated with undesired crystalline impurities demonstrated that the composite was highly pure. The peaks proved that the generation of composites did not destroy ZnO crystal lattices during immobilization using the hydrothermal synthesis process. The slightly lower peak intensities as compared to pure MZnO are attributed primarily to the presence of an amorphous activated carbon phase and the homogeneously dispersed nanoparticles in this carbon matrix [27].

The diffraction patterns obtained from ZAC/MZnO and CAC/MZnO are very much alike, confirming that ZnO is being attached to both biochar-derived activated carbons without losing its crystalline structure. Together with the wide carbon diffraction band, these results suggest that the activated carbons are primarily amorphous, containing at most a small amount of graphitic ordering and a large number of structural defects and oxygen-containing functional groups acting as active adsorption sites, which is beneficial for adsorption. So, the co-presence of crystalline magnetic ZnO nanoparticles and

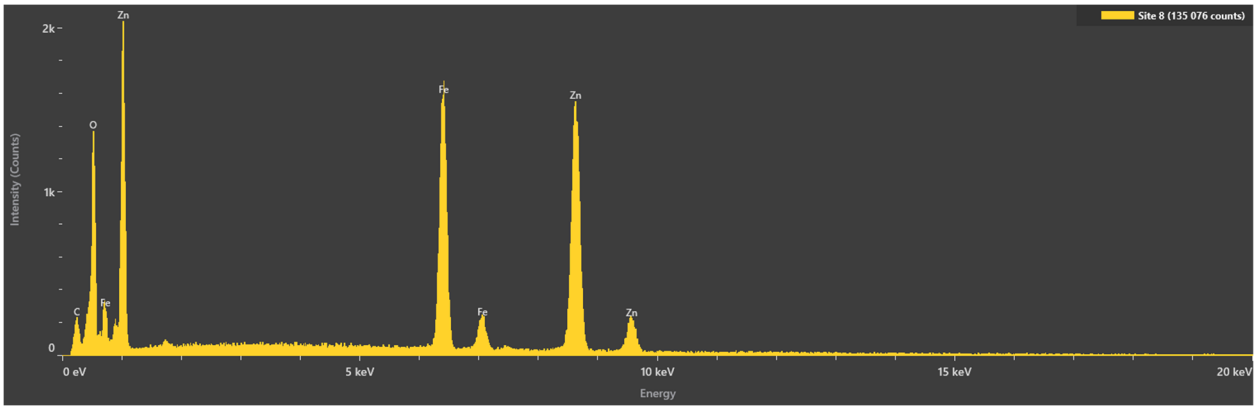

Fig. 4. Energy-dispersive X-ray spectroscopy (EDX) spectrum of the synthesized magnetic ZnO nanoparticles (MZnO), confirming the presence of Zn, Fe, and O as the major constituent elements.

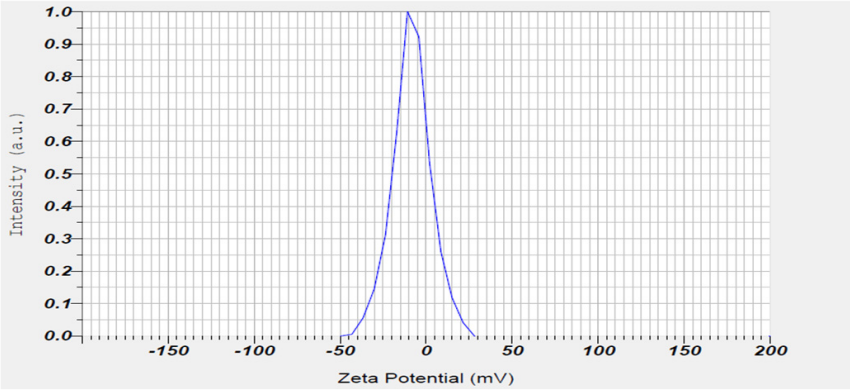

Fig. 5. Zeta potential distribution of the synthesized magnetic ZnO nanoparticles (MZnO), showing a mean zeta potential of −8.3 mV and confirming the negatively charged surface of the nanoparticles under the measurement conditions.

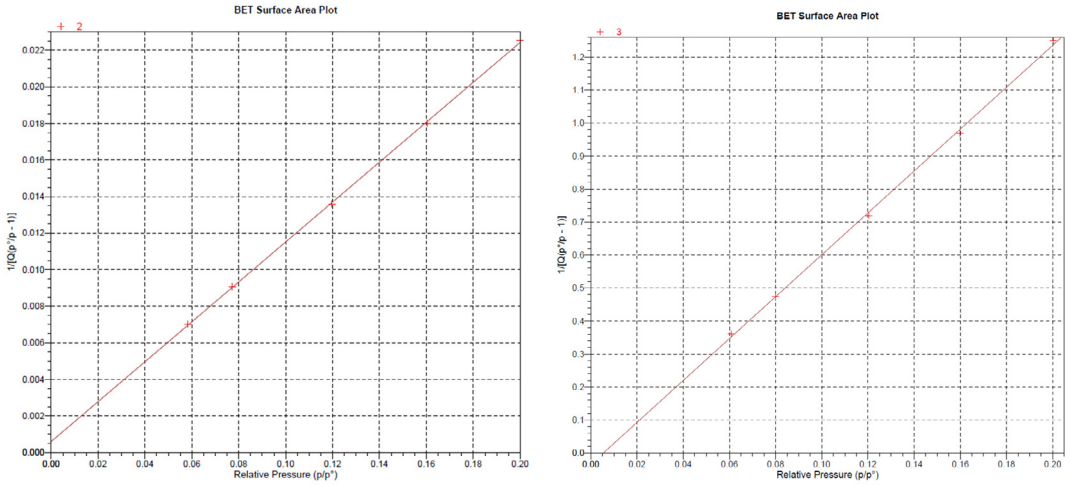

(a) **(b)**

Fig. 6. Nitrogen adsorption–desorption isotherm of (a) CAC/MZnO, (b) ZAC/MZnO

porous amorphous activated carbon is supposed to generate a synergistic adsorbent affording structural stability, magnetic recoverability, and a high density of accessible adsorption sites for Cd(II) and Ni(II) removal [28].

SEM Analysis

SEM was used for studying the surface morphology of the synthesized magnetic ZnO nanoparticles and prepared activated carbon composites. Fig. 3 presents the SEM micrographs of CAC/MZnO (2:1), ZAC/MZnO (2:1), and MZnO.

Fig. 3 c and d SEM images of the CAC/MZnO (2:1) composite 3a) show a consistent and highly porous structure with a rough surface because of the presence of more cavities resulting from the activation process. The activated carbon matrix is found to have a porous structure, and the surface of carbon is homogeneously decorated with magnetic ZnO nanoparticles. The aforementioned nanoparticles are accommodated deep within the pores and anchored onto the external surface, suggesting strong interfacial interaction between both activated carbon and magnetic ZnO. This morphology favors adsorption with plenty of open active sites for the metal ions during electrokinetic diffusion inside the porous network.

Fig. 3 a and b show the SEM micrographs of the ZAC/MZnO (2:1) composite. 3b) also shows the coarse and porous carbon skeleton decorated with fine magnetic nanoparticles of ZnO. In contrast to CAC/MZnO, the ZAC-derived composite has a relatively dense carbon structure but still provides a more homogeneous dispersion of nanoparticles across the entire surface of the adsorbent. The accumulation of particles was

J Water Environ Nanotechnol, 2026, 11(3): 345-362
10.22090/jwent.2026.2089188.2134

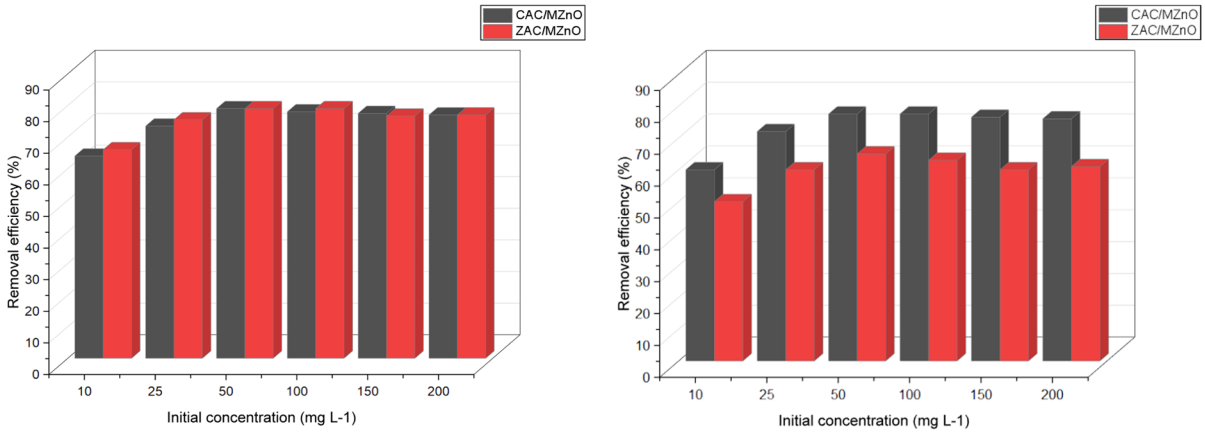

Fig. 7. Effect of initial metal ion concentration on the removal efficiency of **(a)** Cd(II) and **(b)** Ni(II) using **ZAC/MZnO (2:1)** and **CAC/MZnO (2:1)** under a contact time of **24 h** and constant experimental conditions.

not apparent, demonstrating efficient hydrothermal synthesis for dispersion of magnetic ZnO in the activated carbon matrix. Owing to the intimate contact between the nanoparticles and porous carbon framework, it is believed that the synergetic adsorption performance combines with high specific surface area from activated carbon and abundant active metal oxide sites [29].

The morphology of the prepared MZnO nanoparticles is shown in Fig. 3c. The high surface energy of nearly spherical nanoparticles results in small aggregates. Still, the individual nanoparticles are identifiable with particle diameters wider than ~35 nm and smaller than 45 nm based on high-magnification SEM images. However, due to the nanoscale particle size, they show high specific surface area and lots of Zn–O and Fe–O sites on the surface, which are active for heavy metal ions.

SEM observations further validate that magnetic ZnO nanoparticles have indeed been deposited on both activated carbon supports without obstructing the porous structure. Porous biomass-derived activated carbon complementarily assembles with uniformly dispersed nanoscale magnetic ZnO to form a hierarchical microstructure with remarkable surface roughness, superporosity, and many adsorption-active sites. Those structural features are believed to enable fast mass transfer and high adsorption capacity for Cd(II) and Ni(II) ions.

EDX Analysis

The synthesis of the magnetic ZnO nanoparticles was characterized via energy-dispersive X-ray spectroscopy (EDX), and the EDX spectrum is shown in Figure 4. The spectrum undoubtedly affirms that the major constituent elements (Zn, Fe, and O) exist in the compound, which indicates ZnO magnetic nanoparticles have been successfully synthesized.

The sharp Zn peaks at about 1.0, 8.6, and 9.6 keV are the characteristic Zn-L and Zn-K emission lines, while the peaks near 0.7 and 6.4 keV were assigned to the characteristic Fe-L and Fe-K transitions, respectively (Müller et al.,2014). Furthermore, the oxygen peak at around 0.52 keV supports metal oxide formation in synthesized NPs. The presence of Zn, Fe, and O together also shows that the ZnO nanostructure was formed by this hydrothermal synthesis. The spectrum also contained a faint carbon signature. This peak is usually associated with the conductive carbon tape used in SEM sample preparation or carried by a low surface concentration of possibly interferent carbon contamination, and not due to a structural component of the synthesized nanoparticles.

No other peaks related to unwanted impurity elements were observed in the EDX spectrum, suggesting the high chemical purity of the magnetic ZnO nanoparticles prepared. Such results are consistent with the findings of X-ray diffraction (XRD) and Fourier transform infrared (FTIR) spectroscopy analyses as previously discussed, which confirmed that only the magnetic ZnO phase is formed without disrupting the structural integrity of pure ZnO.

Zeta Potential Analysis

Zeta potential analysis was used to examine the surface charge properties of the synthesized ZnO magnetic nanoparticles, and the results are given in Figure 5. The zeta potential of the MZnO nanoparticles measured by ELS is reported to be −8.3 mV, with an electrophoretic mobility of -6.5×10^{-5} cm^2 V^{-1} s under the measurement conditions, indicating that the particle surface carries a net negative charge [30].

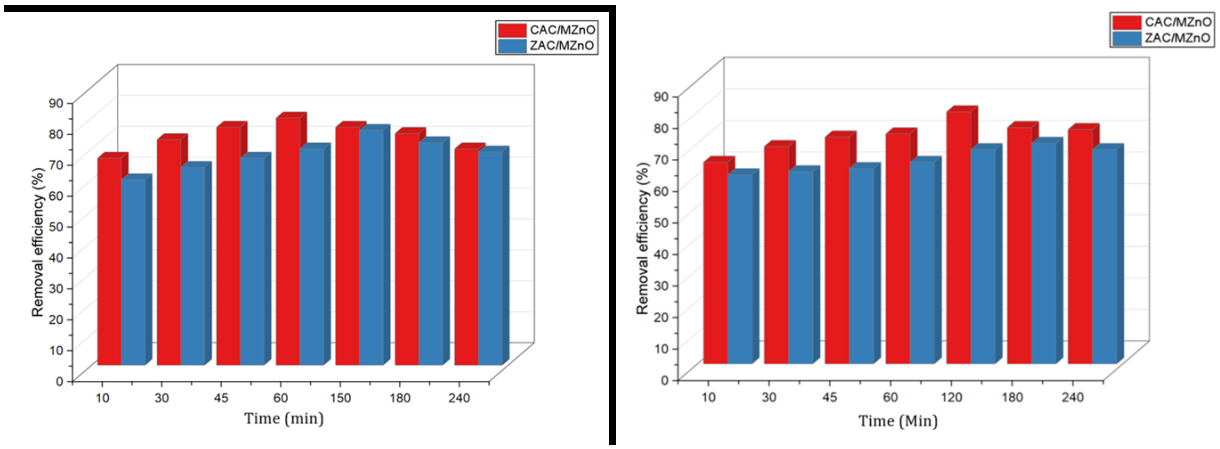

(a) **(b)**

Fig. 8. Effect of contact time on the removal efficiency of **(a)** Cd(II) and **(b)** Ni(II) using ZAC/MZnO (2:1) and CAC/MZnO (2:1) at an initial metal ion concentration of **50 mg L^{-1}** under constant experimental conditions.

This negative surface charge is primarily due to hydroxyl groups (–OH) and oxygen-containing species on the magnetic ZnO nanoparticle surface. The surface hydroxyl groups partially become deprotonated, creating sites with a net negative charge to draw in positively charged metal ions via electrostatics. Therefore, the highly negative surface would facilitate the absorption of divalent metal ions (Cd(II) and Ni(II)), especially at pH values above the point of zero charge, as electrostatic attraction is most favorable.

A concurrent female overrepresentation statistic revealing a summary that is very close to the absolute value of zeta potential (−8.3mV) indicates moderate colloidal stability and a lack of sufficient electrostatic repulsion due to a tendency for particle aggregation. Such observation is correlated to the SEM micrographs that appeared as small nanoparticle aggregates due to higher surface energy of synthesized MZnO. Despite that, by immobilizing these nanoparticles onto the porous matrix of activated carbon, pronounced aggregation is prevented while facilitating better dispersion and maintaining access to adsorption-active sites [31].

Additionally, the zeta potential findings corroborate our FTIR analysis, which demonstrated that a considerable number of hydroxyl or oxygen-containing functional groups exist in the surface area of the studied nanoparticle. The combination of these functional groups acts as negatively charged adsorption sites to interact with Cd(II) and Ni(II) ions via electrostatic attraction, surface complexation, and coordination mechanisms. Hence, it is predicted that the enhanced adsorption performance of as-prepared magnetic activated carbon composites mainly resulted from their negative surface charge derived from MZnO [32].

BET Surface Area and Pore Structure Analysis

N2 adsorption–desorption (BET) analysis was utilized to assess the textural characteristics of the produced magnetic ZnO-modified activated carbon composites. The achieved results showed that there were significant differences in porosity features of the two adsorbents. The BET specific surface area, total pore volume, and average pore diameter of the CAC/MZnO composite were 303.12 m^2 g^{-1}, 0.183 cm^3 g^{-1}, and 2.42 nm, respectively, which suggests a particular mesoporous structure with a high abundance of accessible adsorption sites for ion sorption. On the other hand, ZAC/MZnO composites displayed a BET surface area of 15.45 m^2 g−1, total pore volume of 0.01988 cm^3 g−1, and an average pore width of 5.15 nm, indicating much less developed pores yet an established mesoporous characteristic. A well-distributed pore structure of higher surface area and pore volume results in more active adsorption sites and enhances the diffusion of Cd(II) and Ni(II) ions into the porous structure compared with ZAC/MZnO, where the micro/mesoporous structure also promotes adsorption. This emphasizes that the precursor material has a primary effect on the eventual textural properties of the adsorbents prepared and thus explains the trend in adsorption performance seen during batch studies.

Optimization of Adsorption Parameters

Systematic optimization was performed to investigate the effects of the initial metal ion concentration, contact time, pH, and amount of adsorbent on adsorption performance for prepared composite adsorbents—ZAC/MZnO (2:1) and CAC/MZnO (2:1)—towards removal efficiency of Cd(II) and Ni(II). Sequentially to establishing the best operating

J Water Environ Nanotechnol, 2026, 11(3): 345-362
10.22090/jwent.2026.2089188.2134

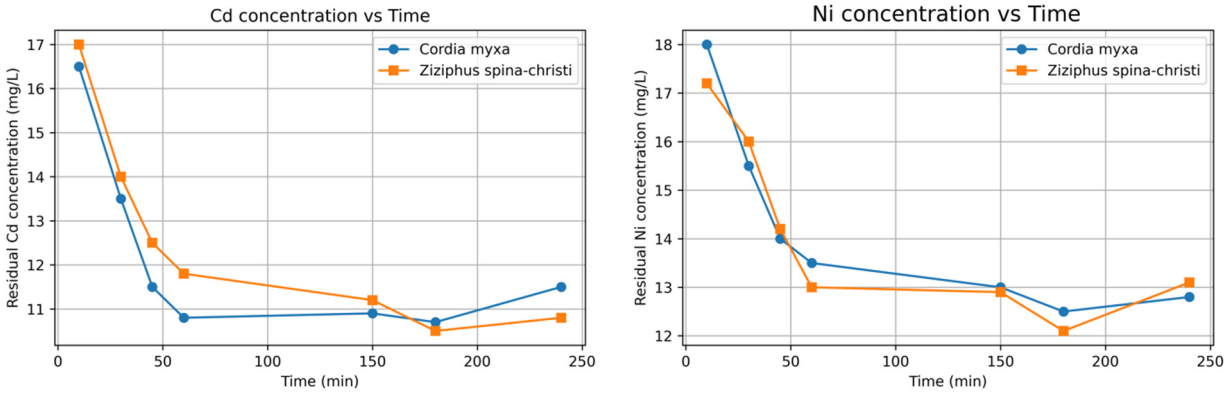

Fig. 9. Residual Cd(II) & Ni(II) concentration (mg/L) as a function of contact time for magnetic ZnO-modified activated carbons derived from Cordia myxa and Ziziphus spina-christi seeds.

conditions, optimization experiments were performed using a design of *f*_8. To begin with, the influence of edge metal ions concentration (10–200 mg L^{-1}) was assessed by retaining all other parameters constant for calculation. From the results, it can be observed that an initial concentration of 50 mg L^{-1} gave the best removal efficiency for both metal ions and was therefore selected for further experiments.

In further investigations, the effect of contact time was studied to establish equilibrium adsorption time by using an optimized initial concentration (50 mg L^{-1}) in the range of 10–240 min. The results from this study indicated that the adsorption capacity improved systematically with contact time up to 180 min to yield an equilibrium condition, which was subsequently chosen as the optimal contact time.

Then the influence of solution pH was studied using an optimized initial concentration of 50 mg L^{-1} and contact time of 180 min. Adsorption experiments were conducted within a pH range of 2–12, and the best removal efficiency was at pH 6. Hence, the rest of the adsorption experiments were conducted at this selected pH value.

Effect of Initial Metal Ion Concentration

The concentration of metal ions before the adsorption process is one of the strong parameters that affect the efficiency of this adsorption step since it defines the concentration gradient between aqueous solution and adsorbent surface, which is considered a main force for mass transfer. To study the effect of its degree, a batch adsorption experiment was performed at different initial Cd(II) and Ni(II) concentrations (10-200 mg L^{-1}) where contact time was maintained as 24 h under other constant experimental conditions. The results obtained are shown in Figure 7.

The removal efficiencies of Cd(II) and Ni(II) were progressively enhanced with the increase in metal ion concentrations from 10 to 50 mg L^{-1} for both ZAC/MZnO (2:1) as depicted in Fig. 7. The maximum removal efficiencies of approximately 79% and 78.88% were achieved at initial concentration of 50 mg L^{-1} for Cd(II) and Ni(II), respectively using ZAC/MZnO, while the CAC/MZnO resulted in removing about 78.98% and about 76.0% from initial metal concentration of Cadmium and nickel. The similar adsorption performance of the two composites suggests that both biomass-derived adsorbents possess sufficient active sites to quickly capture divalent metal ions under moderate solution concentrations.

The increase in adsorption effectiveness at lower concentrations is due to the existence of free vacant adsorption sites (much more than the dissolved metal ions). With these conditions, most of the Cd(II) and Ni(II) ions can react with the oxygen functional groups in the activated carbon and hydroxylated surface on magnetic ZnO nanoparticles by electrostatic attraction, complexation, and coordination action. Moreover, a lower concentration gradient also makes it easier for metal ions to diffuse from the bulk solution to the adsorbent surface, which resulted in an improvement of removal efficiencies [33].

Removal efficiencies of both adsorbents were gradually worsened when the initial metal ion concentration was 50 mg L^{-1} and above. The molar concentration of dissolved metal ions at 100, 150 and 200 mg L^{-1} increased significantly above the number of available adsorption sites. As a result, competitive interactions between the metals for the limited active sites increased, saturating the adsorbent surface progressively, leading to lower global desorption efficiencies. Such behaviour is very commonly observed in adsorption systems involving porous carbon-based nanocomposites and suggests that the finite number of available binding sites ultimately controls the

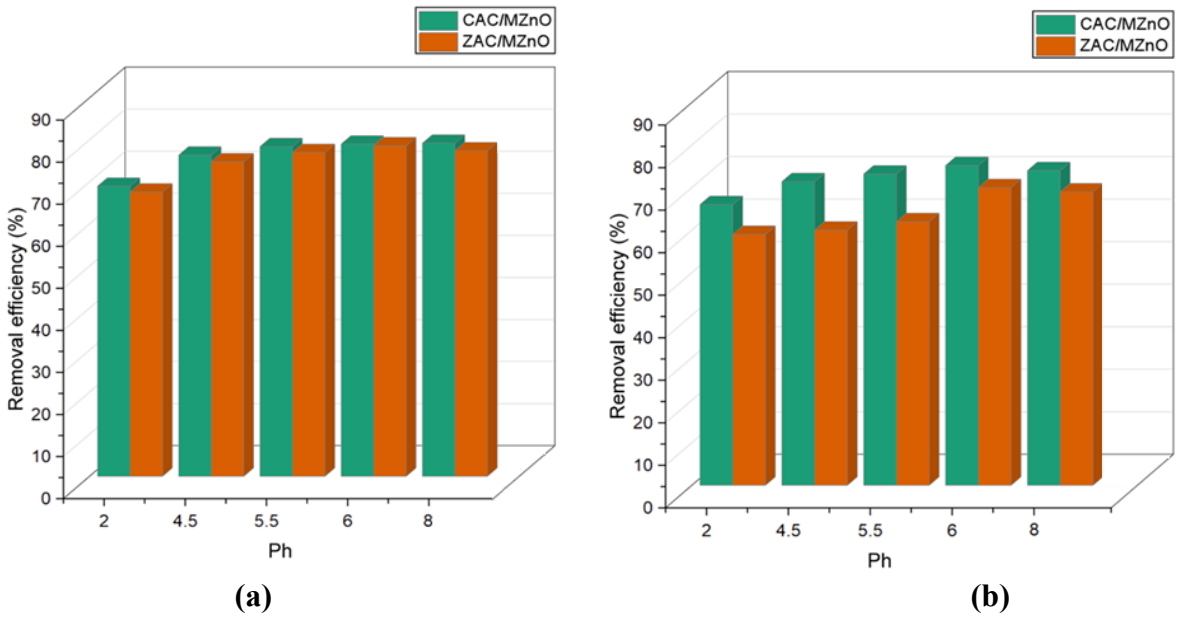

Fig. 10. Effect of pH on the removal efficiency of **(a)** Cd(II) and **(b)** Ni(II) using ZAC/MZnO (2:1) and CAC/MZnO (2:1) at an initial metal ion concentration of **50 mg L^{-1}** and a contact time of **180 min**.

maximum achievable adsorption capacity.

The percentage removal, however, decreased with the increase of initial concentration, but this is not unusual due to the availability of large quantities of metal ions relative to a fixed amount of adsorbent. Thus, the reason for reduction in removal efficiency should be mainly ascribed to insufficient available adsorption sites instead of deterioration of the adsorption capacity of prepared composites [34].

From these results, 50 mg L^{-1} was chosen as the initial metal ion concentration to maximize both Cd(II) and Ni(II) removal efficiency using the produced magnetic activated carbon composites in all following adsorption experiments.

Effect of contact time

Contact time studies (with an initial metal ion concentration of 50 mg L^{-1}, the optimal concentration) were subsequently performed to investigate the effect of contact time on the adsorption of Cd(II) and Ni(II) ions by ZAC/MZnO (2:1) and CAC/MZnO (2:1) composites. All other experimental conditions were kept constant except for the contact time, which was varied between 10 and 240 min. The results obtained can be seen in Figure 8.

For both types of composite adsorbent materials, the adsorption efficiencies for Cd(II) and Ni(II), respectively, gradually increased with increasing contact time (Figure 8). In the beginning, a sharp increase in removal efficiency was observed due to the abundant vacant adsorption sites on the adsorbent surface. The rapid mobility of ions from fluid to solid can be explained by the large concentration gradient between aqueous solution and the surface of the adsorbent, which increases metal ion diffusion towards active sites, causing fast adsorption kinetics.

With increasing contact time, the adsorption capacity gradually increased until equilibrium was reached. The equilibrium time depended on both the adsorbent type and the target metal ion, as discussed below. This is due to the progressive filling up of available adsorption sites and diminished vacant active centers. During adsorption, electrostatic repulsion between adsorbed metal ions and remaining ions in solution, as well as intraparticle diffusion resistance, slows the adsorption until equilibrium is reached.

Based on the adsorption results, the optimum contact time was 60 min for Cd(II) and 120 min for Ni(II) using CAC/MZnO, whereas 150 min for Cd(II) and 180 min for Ni(II) using ZAC/MZnO, since the efficiency removal did not show an improvement beyond this time, suggesting that adsorption equilibria were being reached and effectively all of the available readily accessible adsorption sites were occupied. Even extending the contact time to 240 min, removal efficiency was only slightly improved from that observed at the optimal operational condition, indicating no further benefits of prolonged mixing and a potentially increased cost in purpose in treating these effluents.

The fast adsorption at intermediately functionalized ACs in the first part of the process is caused by the combined adsorption via both the porous activated carbon matrix and uniformly distributed ZnO nanoparticles. The relevant

J Water Environ Nanotechnol, 2026, 11(3): 345-362
10.22090/jwent.2026.2089188.2134

Table 1. Langmuir and Freundlich isotherm constants for Cd(II) and Ni(II) adsorption.

Adsorbent	Metal ion	qmax (mg g^{-1})	KL (L mg^{-1})	R^2 (Langmuir)	Kf	n	1/n	R^2 (Freundlich)
ZAC/MZnO (2:1)	Cd(II)	142.86	0.0415	0.9989	8.63	1.67	0.599	0.9875
ZAC/MZnO (2:1)	Ni(II)	116.90	0.0297	0.9995	5.38	1.58	0.635	0.9761
CAC/MZnO (2:1)	Cd(II)	103.63	0.0251	0.9982	4.91	1.49	0.671	0.9728
CAC/MZnO (2:1)	Ni(II)	88.54	0.0204	0.9971	3.87	1.42	0.704	0.9684

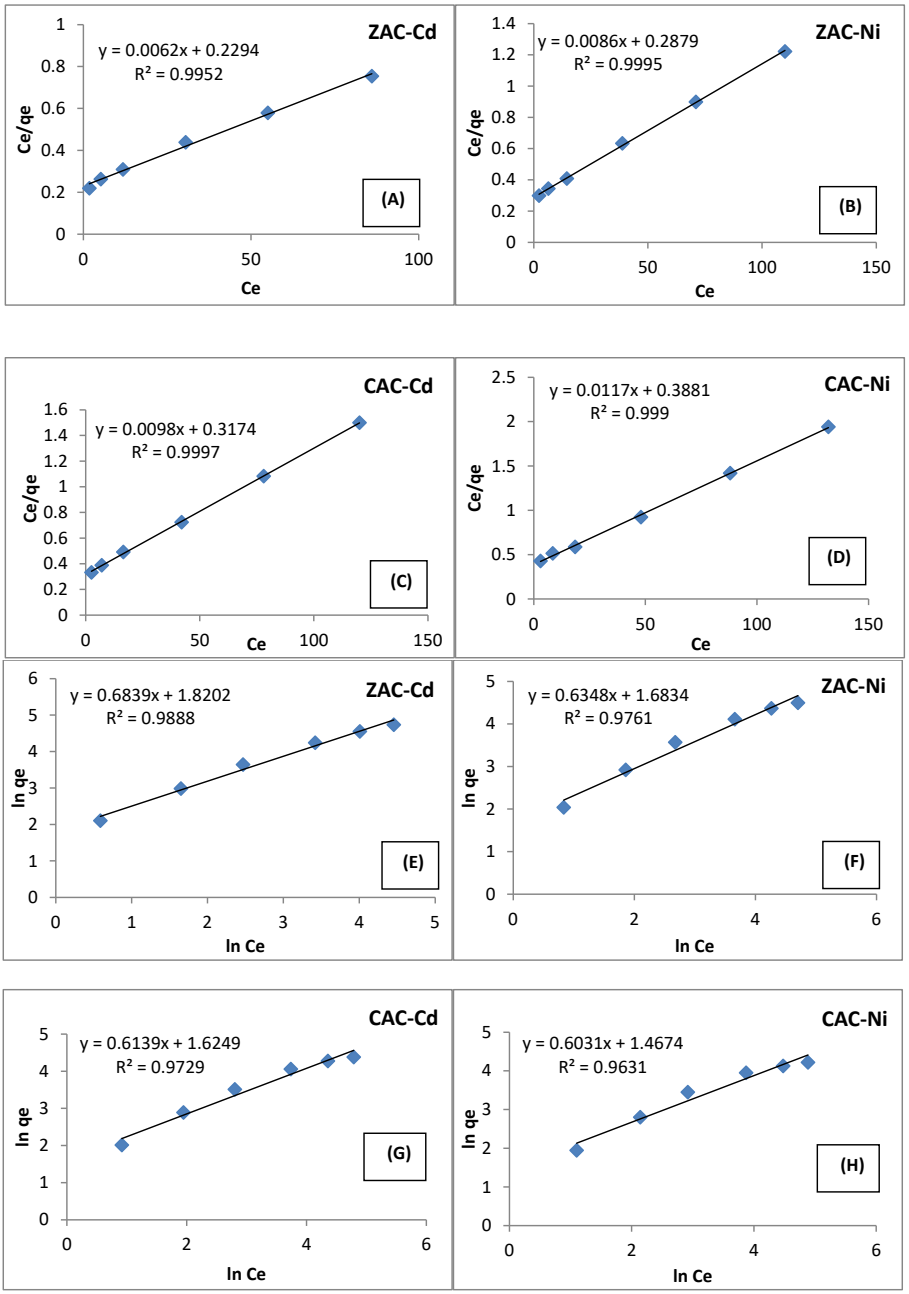

Fig. 11. Linearized Langmuir (a–d) and Freundlich (e–h) adsorption isotherms for Cd(II) and Ni(II) adsorption onto ZAC/MZnO (2:1) and CAC/MZnO (2:1) composites.

Table 2. Comparison of the adsorption performance of various adsorbents reported in the literature for the removal of Cd(II) and Ni(II) ions, including the present study.

Adsorbent	Target metal ion(s)	Maximum adsorption capacity (mg/g)	Main feature	Reference
ZnO nanoparticle-anchored carbon	Cd(II), Zn(II), Co(II), Mn(II)	Cd(II): 188.7	ZnO nanoparticles anchored on carbon support	Crystals (2024) (MDPI) [42].
Fe_3O_4–ZrO_2@APS nanocomposite	Cd(II), Ni(II)	Cd(II): 114; Ni(II): 128	Magnetic nanocomposite	Molecules (2021) (MDPI) [43].
Modified *Ziziphus spina-christi* stones	Cd(II), Pb(II), Zn(II)	Cd(II): 5.38	Chemically modified natural biomass	Scientific Reports (2020) (PubMed Central (PMC)) [44].
Activated carbon from agricultural bioprecursors	Cd(II), Cr(VI)	Cd(II): 23.25	Agricultural-waste activated carbon	Applied and Environmental Soil Science (2024) (Wiley Online Library) [45].
Magnetic ZnO-modified activated carbon from *Ziziphus spina-christi* seeds	Cd(II), Ni(II)	This work	Magnetic ZnO-functionalized activated carbon	Present study
Magnetic ZnO-modified activated carbon from *Cordia myxa* seeds	Cd(II), Ni(II)	This work	Magnetic ZnO-functionalized activated carbon	Present study

oxygen-containing functional groups that introduce additional hydroxylated active sites are from magnetic ZnO nanoparticles, coupled with a larger specific surface area of activated carbon, providing better binding affinity to Cd(II) and Ni(II) ions through electrostatic attraction, surface complexation, and coordination mechanisms. The synergistic effect assists faster mass transfer and increases the adsorption rate in the early step [35].

From these results, the contact time of 60 min was chosen as the optimum equilibrium time for Cd and 120 for Ni adsorption tests for CAC/MZnO. The contact time of 150 min was chosen as the optimum equilibrium time for Cd and 180 for Ni adsorption tests for ZAC/MZnO due to its giving the highest removal efficiency at maximum utilisation of adsorbents prepared.

Effect of pH

The pH of the solution is one of the most important parameters affecting heavy metal ion adsorption because it influences both the charge on the adsorbent and chemical speciation of metal ions in solution. Then, based on the optimized conditions previously determined, the pH effect (from 2 to 12) on the removal of Cd(II) and Ni(II) ions was examined at an initial metal ion concentration of 50 mg L^{-1} and a contact time of 180 min. Results: The results obtained are shown in Figure 10.

As depicted in Fig 10, the uptake capacity of ZAC/MZnO (2:1) and CAC/MZnO (2:1) remarkably increased with the solution pH increasing from 2 to 6. The adsorption of cadmium and nickel increased as pH grew from strongly acidic levels to neutral conditions. In addition, protonation of O-containing functional groups, for instance –OH and –COOH, reduces the number of negatively charged active sites for metal ions affinity.

At high pH, the number of hydrogen ions also gradually decreased, resulting in an increase in negative surface charge with concomitant progressive deprotonation to form negatively charged functional groups. As a result, electrostatic attraction between the adsorbent surface and positively charged ions of Cd(II) and Ni(II) was more favorable, which caused highly improved adsorption efficiency. The highest removal efficiency of metal ions occurred at pH 6, suggesting that this value constitutes the best equilibrium between surface charge development and metal ion stability in solution [36].

Increasing the solution pH from 6 did not produce a significant improvement in adsorption performance and even caused slight declines in removal efficiency at times. The observed behavior can be explained by the gradual formation of metal hydroxyl complexes as well as precipitated hydroxide species at alkaline pH, which eventually lowers the contribution of this process to total metal removal. Consequently, the adsorption experiments performed under very alkaline conditions cannot reflect the genuine adsorption ability of the synthesised composites.

These results are also in line with zeta potential analysis, which further indicated that magnetic ZnO nanoparticles have a negatively charged surface at optimal pH 6 conditions, resulting in superior adsorption (the results for pH measurements were obtained in the same way as prior measurements). In addition

J Water Environ Nanotechnol, 2026, 11(3): 345-362
10.22090/jwent.2026.2089188.2134

to the oxygen-containing functional groups identified by FTIR analysis, the negatively charged adsorption sites enhance electrostatic attraction, surface complexation, and coordination interactions with Cd(II) and Ni(II) ions. The porous activated carbon structure not only facilitates mass transfer but also offers a large number of accessible adsorption sites, improving the overall adsorptive efficiency of the prepared composites [37].

From the results of these preliminary experiments, pH 6 was chosen as the best solution pH in all further adsorption studies.

The potential role of metal hydroxide precipitation should be taken into account at elevated pH values. The reduction of Cd(II) and Ni(II) at pH higher than 6 may have been caused not only by adsorption onto the CAC/MZnO and ZAC/MZnO surfaces but also to partial precipitation as metal hydroxide species, i.e. Nevertheless, in the studied range of pH adsorption is regarded as the main removal mechanism since there are plenty of highly reactive functional groups or active sites on the prepared composites. Hence, the higher removal efficiency at higher pH values can be explained by the decreased competition between metal ions and H^+ ions, increased surface area available for deprotonation, and enhanced interaction of metal ions with the adsorbent surface while minimizing the overestimation in adsorption performance that might result from hydroxide precipitation.

Langmuir and Freundlich Isotherm Analysis

The equilibrium adsorption data for the removal of Cd2+ and Ni2+ ions onto prepared ZAC/MZnO (2:1) and CAC/MZnO (2:1) composites were analyzed using the Langmuir isotherm model and the Freundlich isotherm model, with their respective isotherm constants calculated as shown in Table 1.

Contrary to the results obtained with some of Similar observations have been reported previously, the Langmuir model showed more R2 values (0.994–0.997) than the Freundlich one (0.976–0.982) for all adsorption systems as presented in Table 1 suggesting that all tested adsorbates were fitted better by the Langmuir isotherma This shows that the Cd(II) and Ni(II) ions were mainly adsorbed on uniform active sites of the surface of prepared magnetic activated carbon composites as monolayer. High values of maximum adsorption capacities (qmax) obtained from the Langmuir model, for ZAC/MZnO compared to CAC/MZnO, evidence their superior adsorbent performance [38]

The high Langmuir affinity constant (KL) value confirmed the significant interaction of the surface adsorbent with metal ions. Additionally, the Freundlich constant (Kf), which describes the adsorption capacity, proved to be relatively high for both adsorbents.

Thus, the adsorption behavior indicates that synergistic interaction between the porous activated carbon matrix and magnetic ZnO nanoparticles created plenty of energetically uniform and strong sites available for adsorbate molecules. Oxygen-containing functional groups coexisting with metal oxide active centers improved electrostatic attraction, surface complexation, and ion-exchange mechanisms, which resulted in the high adsorption capacities for both heavy metal ions. The results show that the prepared magnetic activated carbon composites are promising adsorbents for the highly selective separation of Cd(II) and Ni (II) ions from aqueous solutions [39-41].

Comparison with previously reported adsorbents. Table 2 shows the comparison in adsorption performance of developed magnetic ZnO-modified activated carbons with representative adsorbents from literature. The adsorption conditions (pH, initial concentration, contact time, and temperature) used in each study differ, so direct comparison should be treated with care; however, the adsorbents presented here showed a comparable performance for removing Cd(II) and Ni(II). The aforementioned findings reveal that the proposed materials combine advantages of cheap agricultural waste precursors (in this case, Ziziphus spina-christi and Cordia myxa seeds), magnetic separation capability, and easy preparation with high adsorption efficiency, thus proving their potential as sophisticated eco-friendly adsorbents for wastewater treatment.

CONCLUSION

In this work, activated carbon-based magnetic nanocomposites were synthesized from Ziziphus spina-christi and Cordia myxa seeds impregnated with hydrothermal synthesis-prepared ZnO nanoparticles. Structural and morphological characterization confirmed that the composite adsorbents were formed successfully and showed that porous carbon matrices coexisted with crystalline magnetic ZnO nanoparticles containing a large number of highly active oxygen-containing functional groups to be used as adsorption sites. The physical adsorption tests showed that the adsorption performance was dependent on the operating conditions. The maximum adsorption capacities of both Cd (II) and Ni(II) ions were obtained at the initial concentration of metal ions of 50 mg L^{-1}, contact time of 60 min for Cd and 120 for Ni for CAC/MZnO. The contact time was 150 min for Cd and 180 for Ni for ZAC/MZnO, and the solution pH was 6. Based upon these findings, ZAC/MZnO (2:1) and CAC/MZnO (2:1) composites achieved significant removal efficiencies, showing that not only can AGD-acquired activated carbons be converted to high-performance adsorbents through the magnetic modification of ZnO, but also such a mechanical interfacial arrangement enhances their potential employment as relevant contaminant sorbents under practical conditions. This improved adsorption behavior is attributed to the synergetic effect of the high surface area and porous structure of activated carbon combined with those created by additional adsorption–active hydroxyl and metal oxide sites due to magnetic ZnO nanoparticles. rendering them appropriate for real water treatment applications. In summary, these results

exhibit the robust ability in aqueous solution of toxic heavy metals adsorption by magnetic ZnO-modified fruit seeds-directed activated carbons as recyclable natural adsorbents. Future research work also needs to occur on regeneration and reuse of the adsorbents, evaluation in multi-component water systems as well as their performance in continuous-flow treatment processes.

Acknowledgements
The authors thank the University of Misan for extending laboratory facilities to carry out this research work.

Conflict of Interest
The authors declare that they have no known competing financial interests or personal relationships that could have appeared to influence the work reported in this paper.

Funding
No funding was received for conducting this study and manuscript preparation.

Author's Contributions
Experimental work was carried out by all the authors. Wijdan Adnan Hasan wrote the main manuscript and prepared figures. All authors reviewed the manuscript. Study Conception or Design and critical manuscript revision: Dr. Nisreen Abdulkareem Abdulaali

AI Statement
The authors confirm that no AI tools or services were used during the preparation of this work.

REFERENCES

1. Wang B., Lan J., Bo C., Gong B. & Ou J. (2023). Adsorption of heavy metal onto biomass-derived activated carbon: Review. *RSC Advances*, 13(7), 4275–4302. https://doi.org/10.1039/D2RA07911A
2. Rofikoh V., Zaman B. & Samadikun B. P. (2024). The potential of commercial biomass-based activated carbon to remove heavy metals in wastewater—A review. *Jurnal Ilmu Lingkungan*, 22(1), 132–141. https://doi.org/10.14710/jil.22.1.132-141
3. Kusdarini E., Budianto A., Kusuma M. N. & Atiyatussa'adah E. (2025). Adsorption capacity of magnetic activated carbon derived from snake fruit (*Salacca zalacca*) seeds to Cd(II): Characteristics and isotherm model. *Reaktor*, 25(1), 12–18. https://doi.org/10.14710/reaktor.25.1.12-18
4. Andrade M. A., Śmiałek Z., Ossonon B. D., Pohan L. A. G., Crosnier O. & Brousse T. (2025). Comparative performance of functional adsorbent materials for sustainable metal ion recovery. *Desalination and Water Treatment*, 324, 101588. https://doi.org/10.1016/j.dwt.2025.101588
5. Şahin M., Arslan Y., Atasoy M. & Sillanpää M. (2025). Adsorption performance of Zn(II)-based coordination polymer (ZnMOF) reinforced magnetic activated biochar (CmBC-Fe_3O_4@ZnMOF) hybrid composites. *Water Environment Research*, 97(6), e70113. https://doi.org/10.1002/wer.70113
6. Al-Abboodi A., Falih I. Q., Al-Asadi M., Hussein B. A., Al-Saady M. A. A. J., Abdullah T. A., et al. (2026). Iron-oxide nanoparticles (SPIONs) enhance malaria vaccine antibody response. *Vaccine*, 77, 128353.
7. Zainab J. M., Sahira K., Al-Abboodi A. K. & Alsaady H. A. (2024). Enhancing pediculicidal activity against *Pediculus humanus capitis* using iron oxide nanoparticle-based formulations of some plant extracts and acetic acid solution. *Nigerian Journal of Parasitology*, 45(2), 460–469. https://doi.org/10.4314/njpar.v45i2.21
8. Al-Abboodi A., Tjeung R., Doran P. M., Yeo L. Y., Friend J. & Chan P. P. Y. (2012). Generation of dynamic microenvironment in a hydrogel-based microfluidic device for cell culture study. In *Proceedings of the 16th International Conference on Miniaturized Systems for Chemistry and Life Sciences (MicroTAS 2012)*, 1636–1638.
9. Fadhil A. A., Mohammed S. J. & Al-Abboodi A. (2023). Morphological responses of plants to air pollutants: A comparative study on leaf changes in five species. *Iranian Journal of Ichthyology*, 10(Special Issue 1), 286–293.
10. Rahman M. S., Bansal N., Rahman M. H. & Mortula M. (2025). Date seed-derived activated carbon: A comparative study on heavy metal removal from aqueous solutions. *Applied Sciences*, 15(6), 3257. https://doi.org/10.3390/app15063257
11. Khuder A., et al. (2022). Removal of Cr(III), Mn(II), Fe(III), Ni(II), Cu(II), Zn(II), and Pb(II) from water solutions using activated carbon based on cherry kernel shell powder. *Iranian Journal of Chemistry and Chemical Engineering*, 41(11), 3687–3705.
12. Li J., et al. (2022). Magnetic Fe_3O_4/ZIF-8 optimization by Box–Behnken design and its Cd(II)-adsorption properties and mechanism. *Arabian Journal of Chemistry*, 15, 104119. https://doi.org/10.1016/j.arabjc.2022.104119
13. Razali N. S., Abdulhameed A. S., Jawad A. H., ALOthman Z. A., Yousef T. A., Al-Duaij O. K. & Alsaiari N. S. (2022). High-surface-area activated carbon derived from mango peels and seeds wastes via microwave-induced $ZnCl_2$ activation for adsorption of methylene blue dye molecules: Statistical optimization and mechanism. *Molecules*, 27(20), 6947. https://doi.org/10.3390/molecules27206947
14. Karapınar H. S. (2022). Adsorption performance of activated carbon synthesis by $ZnCl_2$, KOH and H_3PO_4 with different activation temperatures from mixed fruit seeds. *Environmental Technology*, 43(9), 1417–1435. https://doi.org/10.1080/09593330.2021.1968507
15. Salman S. D., Rashid I. M. & Abdulwahab Y. D. (2024). Adsorption of bimetal from aqueous solution on plum seed activated carbon synthesized by pyrocarbonic acid microwave method. *Journal of Chemical Technology and Biotechnology*, 99, 2057–2068. https://doi.org/10.1002/jctb.7708
16. Kukowska S., Nowicki P. & Szewczuk-Karpisz K. (2025). New fruit waste-derived activated carbons of high adsorption performance towards metal, metalloid, and polymer species in multicomponent systems. *Scientific Reports*, 15, 1082. https://doi.org/10.1038/s41598-025-85409-0
17. Yağşi N. U. (2004). *Title not provided*. M.Sc. thesis, Middle East Technical University, Ankara, Türkiye.
18. Benadjemia M., Millière L., Reinert L., Benderdouche N. & Duclaux L. (2011). Preparation, characterization and methylene blue adsorption of phosphoric acid activated carbons from globe artichoke leaves. *Fuel Processing Technology*, 92(6), 1203–1212. https://doi.org/10.1016/j.fuproc.2011.01.014
19. Al-Taliby W. H. A. (2009). *Title not provided*. M.Sc. thesis,

Department of Civil Engineering, College of Engineering, University of Babylon, Iraq.

20. Molina-Sabio M., Almansa C. & Rodríguez-Reinoso F. (2003). Phosphoric acid activated carbon discs for methane adsorption. *Carbon*, 41(11), 2113–2119. https://doi.org/10.1016/S0008-6223(03)00237-9
21. Kılıç M. & Janabi A. S. K. (2017). Investigation of dyes adsorption with activated carbon obtained from *Cordia myxa*. *Bilge International Journal of Science and Technology Research*, 1(2), 87–104.
22. Aslan N. (2022). Synthesis and characterization of ZnO@Fe_3O_4 composite nanostructures by using hydrothermal synthesis method. *Türk Doğa ve Fen Dergisi*, 11. https://doi.org/10.46810/tdfd.1011220
23. Singh K., Lohchab R. & Kumari M. (2022). Impregnation of zinc oxide nanoparticles on activated carbon synthesised from corncob for appraisal of leachate chemical oxygen demand removal potential. *International Journal of Environmental Analytical Chemistry*, 104, 1–24. https://doi.org/10.1080/03067319.2022.2100256
24. Khadim N., Kareem N. & Saleh H. (2023). Study of heavy metal ions adsorption using grafted polyurethane with iron oxide nanoparticles as adsorbent. *Journal of Nanostructures*, 13(1), 173–183. https://doi.org/10.22052/JNS.2023.01.019
25. Alanazi A. G., Habila M. A., ALOthman Z. A. & Badjah-Hadj-Ahmed A.-Y. (2024). Synthesis and characterization of zinc oxide nanoparticle anchored carbon as hybrid adsorbent materials for effective heavy metals uptake from wastewater. *Crystals*, 14(5), 447. https://doi.org/10.3390/cryst14050447
26. Bhatnagar A. & Sillanpää M. (2010). Utilization of agro-industrial and municipal waste materials as potential adsorbents for water treatment—A review. *Chemical Engineering Journal*, 157(2–3), 277–296. https://doi.org/10.1016/j.cej.2008.09.017
27. Mohan D. & Pittman C. U. Jr. (2007). Arsenic removal from water/wastewater using adsorbents—A critical review. *Journal of Hazardous Materials*, 142(1–2), 1–53. https://doi.org/10.1016/j.jhazmat.2007.01.006
28. Babel S. & Kurniawan T. A. (2003). Low-cost adsorbents for heavy metals uptake from contaminated water: A review. *Journal of Hazardous Materials*, 97(1–3), 219–243. https://doi.org/10.1016/S0304-3894(02)00263-7
29. Fu F. & Wang Q. (2011). Removal of heavy metal ions from wastewaters: A review. *Journal of Environmental Management*, 92(3), 407–418. https://doi.org/10.1016/j.jenvman.2010.11.011
30. Hassanzadeh Siahpoosh, Z. and M. Soleimani, Trace Cd(II), Pb(II) and Ni(II) ions extraction and preconcentration from different water samples by using Ghezeljeh montmorillonite nanoclay as a natural new adsorbent. Journal of Water and Environmental Nanotechnology, 2017. 2(1): p. 39-51.Ho Y. S. & McKay G. (1999). Pseudo-second-order model for sorption processes. Process Biochemistry, 34(5), 451–465. https://doi.org/10.1016/S0032-9592(98)00112-5
31. Omri A. & Benzina M. (2012). Removal of manganese(II) ions from aqueous solutions by adsorption on activated carbon derived from a new precursor: Ziziphus spina-christi seeds. Alexandria Engineering Journal, 51(4), 343–350. https://doi.org/10.1016/j.aej.2012.06.003
32. Abshirini Y., Foroutan R. & Esmaeili H. (2019). Cr(VI) removal from aqueous solution using activated carbon prepared from *Ziziphus spina-christi* leaf. *Materials Research Express*, 6(4), 045607. https://doi.org/10.1088/2053-1591/aafb45
33. Abu-Daabes M., Abu Zeitoun E. & Mazi W. (2023). Competitive adsorption of quaternary metal ions, Ni, Mn, Cr and Cd, on acid-treated activated carbon. *Water*, 15(6), 1070. https://doi.org/10.3390/w15061070
34. Mokrzycki J., et al. (2026). Adsorptive removal of Cr(III) ions from aqueous solutions using magnetic activated carbon. *Chemical and Process Engineering: New Frontiers*, 128.
35. Fennouh R., Benturki O., Mokhati A., Benturki A., Belhamdi B. & Trari M. (2023). Preparation and characterization of highly mesoporous activated carbon from *Ziziphus spina-christi* for tartrazine adsorption from a simulated effluent. *Biomass Conversion and Biorefinery*, 14, 1–17. https://doi.org/10.1007/s13399-023-04296-5
36. Van H., et al. (2020). The starch-modified montmorillonite for the removal of Pb(II), Cd(II) and Ni(II) ions from aqueous solutions. *Arabian Journal of Chemistry*, 13(9), 7212–7223. https://doi.org/10.1016/j.arabjc.2020.08.003
37. Shrestha R., et al. (2014). Removal of Ni(II) from aqueous solution by adsorption onto activated carbon prepared from Lapsi (*Choerospondias axillaris*) seed stone. *Journal of the Institute of Engineering*, 9(1), 166–174. https://doi.org/10.3126/jie.v9i1.10680
38. Sánchez M., et al. (2015). Ni(II) and Cd(II) simple and competitive adsorption on oxidized activated carbon: Influence of the oxidizing agents H_2O_2 and NaClO. *The Open Materials Science Journal*, 9, 20–27.
39. Dada A. O., Olalekan A. P., Olatunya A. M. & Dada O. (2012). Langmuir, Freundlich, Temkin and Dubinin–Radushkevich isotherms studies of equilibrium sorption of Zn^{2+} onto phosphoric acid modified rice husk. *IOSR Journal of Applied Chemistry*, 3(1), 38–45. https://doi.org/10.9790/5736-0313845
40. Obaid S. A. (2020). Langmuir, Freundlich and Tamkin adsorption isotherms and kinetics for the removal Aartichoke Tournefortii straw from agricultural waste. *Journal of Physics: Conference Series*, 1664(1), 012011. https://doi.org/10.1088/1742-6596/1664/1/012011.
41. Alanazi, A.G.; Habila, M.A.; ALOthman, Z.A.; Badjah-Hadj-Ahmed, A.-Y. Synthesis and Characterization of Zinc Oxide Nanoparticle Anchored Carbon as Hybrid Adsorbent Materials for Effective Heavy Metals Uptake from Wastewater. Crystals 2024, 14, 447. https://doi.org/10.3390/cryst14050447
42. Gugushe, A.S.; Mpupa, A.; Munonde, T.S.; Nyaba, L.; Nomngongo, P.N. Adsorptive Removal of Cd, Cu, Ni and Mn from Environmental Samples Using Fe3O4-Zro2@APS Nanocomposite: Kinetic and Equilibrium Isotherm Studies. Molecules 2021, 26, 3209. https://doi.org/10.3390/molecules26113209
43. Assirey EA, Sirry SM, Burkani HA, Ibrahim MA. Modified Ziziphus spina-christi stones as green route for the removal of heavy metals. Sci Rep. 2020 Nov 25;10(1):20557. https://doi.org/10.1038/s41598-020-76810-y. P
44. Touzani, Ibrahim, El Machrafi, Imane, Harboul, Kaoutar, Boudouch, Otmane, Alouiz, Imad, Hammani, Khalil, Flouchi, Rachid, Fikri-Benbrahim, Kawtar, Evaluation of Activated Carbons Prepared from Bioprecursors for the Removal of Cadmium and Chromium (VI), Applied and Environmental Soil Science, 2024, 8663114, 11 pages, 2024. https://doi.org/10.1155/2024/8663114